Characteristics of SINR and Ergodic Capacity for MIMO-Based Vehicular VLC

Nan An, Fang Yang, *Senior Member, IEEE*, Ling Cheng, *Senior Member, IEEE*, Jian Song, *Fellow, IEEE*, and Zhu Han, *Fellow, IEEE*

***Abstract*—In response to the shortcomings existing in radio frequency vehicular communications, vehicular visible light communication (VVLC) provides a viable alternative. However, the fluctuation of optical intensity induced by atmospheric turbulence (AT) adversely affects the communication performance of VVLC. In this letter, multi-input multi-output (MIMO) VVLC is employed to enhance communication performance by leveraging diversity. Since the probability distribution of signal-to-interference-plus-noise ratio (SINR) for MIMO-based VVLC is difficult to formulate, a weighted two-step approximation (WTA) method is proposed to approximate it with a log-normal distribution. Subsequently, the ergodic capacity is calculated by the Gauss-Hermite quadrature. Simulation results show that the log-normal distribution obtained by the proposed WTA method effectively approaches the SINR distribution, thus ensuring the accuracy of the ergodic capacity.**

***Index Terms*—MIMO, visible light communication, atmospheric turbulence, Gauss-Hermite quadrature.**

I. Introduction

THE GROWING necessity to improve traffic efficiency and safety has directed substantial focus towards vehicle-to-everything (V2X) communication. While several radio frequency technologies have been proposed for V2X communication, their efficacy remains constrained by limited spectrum availability and the presence of inter-vehicle interference. To address these challenges, vehicular visible light communication (VVLC) emerges as a promising alternative for V2X communication [1], [2].

Manuscript received 26 August 2023; revised 19 November 2023; accepted 14 December 2023. Date of publication 20 December 2023; date of current version 8 March 2024. This work was supported in part by the Academician Expert Open Fund of Beijing Smart-Chip Microelectronics Technology Company Ltd., and in part by the National Key Research and Development Program of China under Grant 2022YFE0101700. The associate editor coordinating the review of this article and approving it for publication was Z. Chang. *(Corresponding author: Jian Song.)*

Nan An and Fang Yang are with the Department of Electronic Engineering, Beijing National Research Center for Information Science and Technology, Tsinghua University, Beijing 100084, China, and also with the Key Laboratory of Digital TV System of Guangdong Province and Shenzhen City, Research Institute of Tsinghua University in Shenzhen, Shenzhen 518057, China (e-mail: an21@mails.tsinghua.edu.cn; fangyang@tsinghua.edu.cn).

Ling Cheng is with the School of Electrical and Information Engineering, University of the Witwatersrand, Johannesburg 2050, South Africa (e-mail: ling.cheng@wits.ac.za).

Jian Song is with the Department of Electronic Engineering, Beijing National Research Center for Information Science and Technology, Tsinghua University, Beijing 100084, China, and also with the Shenzhen International Graduate School, Tsinghua University, Shenzhen 518055, China (e-mail: jsong@tsinghua.edu.cn).

Zhu Han is with the Department of Electrical and Computer Engineering, University of Houston, Houston, TX 77004 USA, and also with the Department of Computer Science and Engineering, Kyung Hee University, Seoul 446-701, South Korea (e-mail: hanzhu22@gmail.com).

Digital Object Identifier 10.1109/LWC.2023.3345005

Numerous studies have been conducted on the VVLC channel model to evaluate the VVLC performance. Despite the prevalence of the Lambertian radiation model in visible light communication (VLC), it falls short of capturing the asymmetry of vehicle lighting modules [1]. By employing the ray-tracing approach, a path loss model of VVLC was developed in [3] that integrated the influence of asymmetric lighting patterns, weather effects, and road reflection. In [4], the channel model considered fluctuations in optical intensity attributed to atmospheric turbulence (AT) and the aforementioned factors, while ignoring interference from other vehicles.

Signal-to-interference-plus-noise ratio (SINR) is an essential metric in appraising the quality of a VVLC link, thus affecting subsequent system decisions including resource allocation [5], [6]. Considering the random fluctuations of optical intensity caused by AT, SINR in VVLC becomes a random variable (RV), whose statistical property is imperative for enhancing VVLC performance. The statistical property of SINR is characterized by the probability density function (PDF) and is difficult to formulate. The SINR characterization of a rate-splitting multiple access system under oceanic turbulence was studied in [7], where the interference and signal originated from the same transmitter, without including interference from external sources. In [8], [9], multi-input multi-output (MIMO) was employed in VVLC to enhance the bit error rate, whereas the effects of AT were lack of consideration.

In this letter, MIMO is considered to reduce the adverse effects of AT on VVLC. The SINR characteristic is explored first to evaluate the performance of MIMO-based VVLC. To approximate the SINR PDF, a weighted two-step approximation (WTA) method is proposed. On this basis, Gauss-Hermite quadrature (GHQ) is utilized to calculate the ergodic capacity (EC) of VVLC. Simulation results verify the effectiveness of the proposed WTA method and the resulting EC, and affirm the efficacy of MIMO in improving the VVLC performance under the influence of AT.

Notation: The expectation and variance are denoted by $\mathbb{E}[\cdot]$ and $\mathbb{D}[\cdot]$, respectively. An RV that follows a normal distribution with an expectation of μ and a variance of σ^2 is represented as $\cdot \sim \mathrm{N}(\mu, \sigma^2)$. Similarly, an RV that follows a log-normal distribution is represented as $\cdot \sim \mathrm{LN}(\mu_1, \sigma_1^2)$, wherein the natural logarithm of the variable follows $\mathrm{N}(\mu_1, \sigma_1^2)$. The Gaussian Q-function is demonstrated as $Q(\cdot)$.

II. System Model

As illustrated in Fig. 1, the scenario of a multi-lane road is considered. VVLC links are established employing light-emitting diodes (LEDs) as transmitters and photodiodes

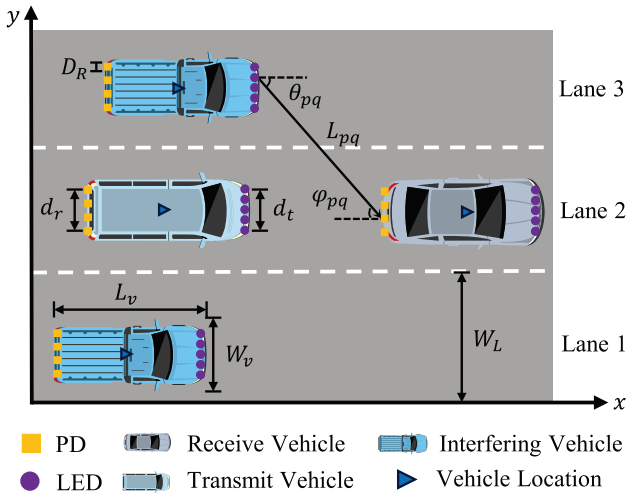

Fig. 1. Vehicle-to-vehicle communication scenario of MIMO-based VVLC.

(PDs) as receivers. Each vehicle is equipped with N_t LEDs at the front and N_r PDs at the rear. An intended VVLC link is established between the transmit vehicle (Tx) and the receive vehicle (Rx), while optical signals emitted by other vehicles are treated as interference. Since VVLC relies on line-of-sight (LOS) links, obstacles between the LED and the PD obstruct the corresponding VVLC link. Besides, in order to represent interference received by Rx concisely, sets of interfering vehicles (IVs) are denoted as $\mathbf{\Phi}_{pq}$, where $p \in \{1, 2, \ldots, N_t\}$ and $q \in \{1, 2, \ldots, N_r\}$, with each set consisting N_{pq} vehicles. For any vehicle $\mathbf{\Phi}_{pq}[i] \in \mathbf{\Phi}_{pq}$, where $i \in \{1, 2, \ldots, N_{pq}\}$, the LOS link between its p-th LED and the Rx's q-th PD remains unobstructed, thus resulting in interference for the Rx.

Assuming a MIMO-based VVLC system with equal gain combining, the received signal of Rx is given by

$$y = \sum_{p=1}^{N_t}\sum_{q=1}^{N_r} h_{pq,T} x_T + \sum_{p=1}^{N_t}\sum_{q=1}^{N_r}\sum_{i=1}^{N_{pq}} h_{pq,i} x_i + \sum_{q=1}^{N_r} w_q, \quad (1)$$

where w_q denotes the additive white Gaussian noise with a zero mean and a variance of σ_0^2 for the q-th PD of Rx. Since w_q has an independent, identically distributed (i.i.d.) characteristic, the total noise w is expressed as

$$w \triangleq \sum_{q=1}^{N_r} w_q \sim N\left(0, N_r\sigma_0^2\right). \quad (2)$$

Besides, x_T and x_i refer to the transmitted signals of Tx and $\mathbf{\Phi}_{pq}[i]$, respectively. $h_{pq,T}$ and $h_{pq,i}$ represent the channel coefficients between the p-th LED of the Tx and the q-th PD of the Rx, and between the p-th LED of $\mathbf{\Phi}_{pq}[i]$ and the q-th PD of the Rx, respectively. For simplicity, subscripts T and i are omitted in the remainder of Section II. The unified model of $h_{pq,T}$ and $h_{pq,i}$ is given by

$$h_{pq} = \eta_q h_{att,pq} h_{tur,pq}, \quad (3)$$

where $h_{att,pq}$ represents the attenuation caused by geometric loss and weather effects, and $h_{tur,pq}$ denotes the impact of AT. η_q is a combined coefficient, including the voltage-current transfer and the PD responsivity. In [3], an attenuation model for the VVLC channel was provided as

$$h_{att,pq} = \left(\frac{D_R}{\xi}\right)^2 \frac{\left(\cos(\theta_{pq})\right)^{2/\varepsilon}}{L_{pq}^2} \exp\left(-\lambda L_{pq}\right), \quad (4)$$

where the correction coefficients ξ and ε, and the extinction coefficient λ exhibit weather-dependent behavior. D_R refers to the aperture diameter of PD. The irradiance angle θ_{pq}, incidence angle φ_{pq}, and propagation distance L_{pq} are parameters that can be measured by sensors such as cameras and lidar, thus $h_{att,pq}$ is easily estimated when the vehicles are moving.

The log-normal distribution is adopted to represent the PDF of AT influence [10], such that $h_{tur,pq} \sim \mathrm{LN}(\mu_{tur,pq}, \sigma_{tur,pq}^2)$. The $\mu_{tur,pq}$ and the PDF of $h_{tur,pq}$ are demonstrated as

$$\mu_{tur,pq} = -\frac{1}{2}\sigma_{tur,pq}^2, \quad (5)$$

$$f_{h_{tur,pq}}(h) = \frac{1}{h\sqrt{2\pi\sigma_{tur,pq}^2}} \exp\left[-\frac{\left(\ln(h) - \mu_{tur,pq}\right)^2}{2\sigma_{tur,pq}^2}\right]. \quad (6)$$

Generally, ensuring that the distance between PDs exceeds the transverse coherence distance is straightforward, which implies that PDs receive uncorrelated signals. Hence, the impact of AT is i.i.d. across various VVLC links. By a variable substitution, it can be shown that h_{pq} also follows a log-normal distribution of $\mathrm{LN}(\mu_{tur,pq} + \ln(\eta_q h_{att,pq}), \sigma_{tur,pq}^2)$. Since the AT influence only depends on the spatial distribution of turbulent eddies, $h_{tur,pq}$ is independent of vehicle mobility.

III. SINR Distribution

The Fenton-Wilkinson (FW) and Schwartz-Yeh (SY) methods for approximating the PDF of a log-normal sum are introduced first. However, the FW and SY methods are not applicable when the components of the log-normal sum have large and small variances, respectively [11], [12]. Hence, the WTA method is proposed to approximate the SINR PDF by comprehensively utilizing the results of the two methods.

A. Fenton-Wilkinson and Schwartz-Yeh Method

Due to the challenge of obtaining the exact closed-form PDF expression of a log-normal sum, many works have utilized a log-normal RV to approximate it, including the FW method [11] and the SY method [11], [13].

In the FW method, central moment matching is employed to calculate the distribution parameters of the approximated log-normal RV. For a log-normal RV $\gamma \sim \mathrm{LN}(\mu_\gamma, \sigma_\gamma^2)$, its expectation and variance are given by

$$\mathbb{E}[\gamma] = e^{\mu_\gamma + \sigma_\gamma^2/2}, \quad (7)$$

$$\mathbb{D}[\gamma] = e^{2\mu_\gamma + \sigma_\gamma^2}\left(e^{\sigma_\gamma^2} - 1\right). \quad (8)$$

When approximating a log-normal sum with γ, the expectation and the variance of the log-normal sum are aligned with $\mathbb{E}[\gamma]$ and $\mathbb{D}[\gamma]$, respectively. These values can be calculated based on the distribution of each component. Thus μ_γ and σ_γ^2 are obtained by

$$\sigma_\gamma^2 = \ln\left(\frac{\mathbb{D}[\gamma]}{\mathbb{E}^2[\gamma]} + 1\right), \quad (9)$$

$$\mu_\gamma = \ln(\mathbb{E}[\gamma]) - \frac{1}{2}\sigma_\gamma^2. \quad (10)$$

The SY method was introduced [11] to recursively calculate the PDF of a log-normal sum. In each recursive step, the sum distribution of two independent log-normal RVs is approximated by another log-normal RV. In order to approximate the sum distribution of correlated log-normal variables, the extension of the SY method was proposed in [13].

B. Proposed Weighted Two-Step Approximation Method

In MIMO-based VVLC, the SINR for the communication link between Tx and Rx is represented as

$$\mathrm{SINR} = \frac{\sum_{p=1}^{N_t}\sum_{q=1}^{N_r}\left(h_{pq,T}P_T\right)^2}{\sum_{p=1}^{N_t}\sum_{q=1}^{N_r}\sum_{i=1}^{N_{pq}}\left(h_{pq,i}P_i\right)^2 + N_r\sigma_0^2}, \quad (11)$$

where P_T and P_i are the transmitted power of each LED in the Tx and $\mathbf{\Phi}_{pq}[i]$, respectively. Since the moments' value of SINR is difficult to calculate, it is hard to approximate SINR PDF directly by the moment matching method. For ease of analysis, $\alpha_{pq,i} \triangleq (h_{pq,i}P_i)^2$ and $\alpha_{pq,T} \triangleq (h_{pq,T}P_T)^2$ are defined. On account of the property of log-normal distribution, it is evident that $\alpha_{pq,i}$ and $\alpha_{pq,T}$ also follow the log-normal distributions, whose distribution parameters are calculated as

$$\mu_{\alpha,pq,T} = 2\mu_{tur,pq,T} + 2\ln\left(\eta_q h_{att,pq,T}P_T\right), \quad (12)$$
$$\sigma^2_{\alpha,pq,T} = 4\sigma^2_{tur,pq,T}, \quad (13)$$
$$\mu_{\alpha,pq,i} = 2\mu_{tur,pq,i} + 2\ln\left(\eta_q h_{att,pq,i}P_i\right), \quad (14)$$
$$\sigma^2_{\alpha,pq,i} = 4\sigma^2_{tur,pq,i}. \quad (15)$$

Due to multiple summations and division in (11), it is challenging to directly calculate the closed-form PDF of SINR, and thus WTA method is proposed to provide an approximate distribution. The numerator of (11) is denoted as $\alpha \triangleq \sum_{p=1}^{N_t}\sum_{q=1}^{N_r}\alpha_{pq,T}$, which is the sum of several independent log-normal RVs, and its central moments are calculated in the Appendix. In the first approximation step of the WTA method, α is approximated by a log-normal RV, whose distribution parameters μ_α and σ_α^2 are calculated by the FW and SY methods. As a consequence, Eq. (11) is simplified to

$$\mathrm{SINR} = \left[\sum_{p=1}^{N_t}\sum_{q=1}^{N_r}\sum_{i=1}^{N_{pq}}\frac{\alpha_{pq,i}}{\alpha} + \frac{N_r\sigma_0^2}{\alpha}\right]^{-1}, \quad (16)$$

where $\beta_{pq,i} \triangleq \alpha_{pq,i}/\alpha$ follows a log-normal distribution with parameters $\mu_{\beta,pq,i} = \mu_{\alpha,pq,i} - \mu_\alpha$ and $\sigma^2_{\beta,pq,i} = \sigma^2_{\alpha,pq,i} + \sigma^2_\alpha$. Besides, $\beta_0 \triangleq N_r\sigma_0^2/\alpha$ also follows a log-normal distribution with parameters $\mu_{\beta,0} = \ln(N_r\sigma_0^2) - \mu_\alpha$ and $\sigma^2_{\beta,0} = \sigma^2_\alpha$.

According to the above definitions, the denominator of (16) is denoted as β, which is a sum of correlated log-normal RVs, and its central moments are calculated in the Appendix. Furthermore, in the second approximation step, β is approximated by a log-normal RV utilizing the FW and SY extension methods, leading to approximate distributions given by $\mathrm{LN}(\mu_{\beta,FW}, \sigma^2_{\beta,FW})$ and $\mathrm{LN}(\mu_{\beta,SY}, \sigma^2_{\beta,SY})$, respectively. Since both methods have different applicability scopes, a weighted method is proposed to take advantage of the results of both methods comprehensively. The weight function and the weighted distribution parameters are given by

$$\kappa\left(\sigma^2_{tur}\right) = \frac{1 + 0.05e^{30(\sigma^2_{tur}-0.2)}}{1 + e^{30(\sigma^2_{tur}-0.2)}}, \quad (17)$$
$$\mu_\beta = \kappa\left(\sigma^2_{tur}\right)\mu_{\beta,FW} + \left(1 - \kappa\left(\sigma^2_{tur}\right)\right)\mu_{\beta,SY}, \quad (18)$$
$$\sigma^2_\beta = \kappa\left(\sigma^2_{tur}\right)\sigma^2_{\beta,FW} + \left(1 - \kappa\left(\sigma^2_{tur}\right)\right)\sigma^2_{\beta,SY}. \quad (19)$$

Consequently, the SINR distribution can be approximated by a log-normal distribution of $\mathrm{LN}(-\mu_\beta, \sigma^2_\beta)$. Moreover, the cumulative distribution function (CDF) of SINR is given by

$$F(s) = P(\mathrm{SINR} < s) = Q\left(\frac{-\mu_\beta - \ln(s)}{\sigma_\beta}\right). \quad (20)$$

In VVLC, the communication outage occurs when the SINR falls below the threshold S_{th} due to interference and noise. Therefore, the outage probability in the VVLC channel is denoted as $F(S_{th})$.

IV. Ergodic Capacity

Because of the differences between radio frequency and VVLC systems, the Shannon channel capacity formula cannot be directly applied to VVLC systems [14]. For VLC systems, a lower bound of channel capacity was derived [15] as

$$C = \frac{1}{2}\ln\left(1 + \frac{e}{2\pi}\mathrm{SINR}\right), \quad (21)$$

where e denoted the Euler number. Utilizing variable substitution, the PDF of channel capacity is given by

$$f_C(c) = \frac{2e^{2c}}{(e^{2c}-1)\sqrt{2\pi\sigma^2_\beta}}\exp\left[-\frac{\ln^2\left(2\pi e^{\mu_\beta - 1}\left(e^{2c}-1\right)\right)}{2\sigma^2_\beta}\right]. \quad (22)$$

Consequently, the EC of VVLC can be calculated as

$$\begin{aligned}\overline{C} &= \int_0^\infty \frac{\frac{1}{2}\ln\left(1+\frac{e}{2\pi}s\right)}{s\sqrt{2\pi\sigma^2_\beta}}\exp\left[-\frac{\left(\ln(s)+\mu_\beta\right)^2}{2\sigma^2_\beta}\right]ds \\ &= \frac{1}{2\sqrt{\pi}}\int_{-\infty}^{\infty}\underbrace{\ln\left(1+\frac{\exp\left(\sqrt{2}s\sigma_\beta - \mu_\beta + 1\right)}{2\pi}\right)}_{g(s)}e^{-s^2}ds\end{aligned} \quad (23)$$

Since the integral in (23) is difficult to calculate, the GHQ is utilized to calculate an approximate numerical result as

$$\overline{C} \approx \frac{1}{2\sqrt{\pi}}\sum_{k=1}^{n}A_k g(s_k), \quad (24)$$

where n represents the chosen order of the Hermite polynomial $H_n(s)$. s_k refer to roots of $H_n(s)$, where $k \in \{1, 2, \ldots, n\}$. The associated weights A_k are calculated by

$$A_k = \frac{2^{n-1}n!\sqrt{\pi}}{n^2 H^2_{n-1}(s_k)}. \quad (25)$$

TABLE I
SIMULATION PARAMETERS

Parameter	Value
Lane width W_L	3.75 m
Number of LEDs N_t	2
Distance between LEDs d_t	1.7 m
Number of PDs N_r	2
Distance between PDs d_r	1.7 m
Vehicle size $L_v \times W_v$	4 m×2.2 m
Power of an LED of Tx P_T	10 W
Power of an LED of IV P_i	10 W
Noise power σ_0^2	10^{-8} W
Combined coefficient η_q	0.9 A/W
Aperture diameter of PD D_R	0.03 m
Extinction coefficient λ	7.82×10^{-3}
Correction coefficient ξ	0.16
correction coefficient ε	1.72×10^{-2}

TABLE II
VEHICLE LOCATIONS IN DIFFERENT CASES

	Case I	Case II	Case III
Tx Position	(19 m, $1.5W_L$)	(19 m, $0.5W_L$)	(17 m, $1.5W_L$)
Rx Position	(31 m, $1.5W_L$)	(30 m, $0.5W_L$)	(31 m, $1.5W_L$)
Others Positions	(15 m, $0.5W_L$) (2 m, $0.5W_L$) (3 m, $1.5W_L$) (7 m, $2.5W_L$) (28 m, $2.5W_L$)	(2 m, $0.5W_L$) (3 m, $1.5W_L$) (11 m, $1.5W_L$) (14 m, $2.5W_L$) (28 m, $2.5W_L$)	(15 m, $0.5W_L$) (2 m, $0.5W_L$) (3 m, $1.5W_L$) (8 m, $2.5W_L$) (28 m, $2.5W_L$)

V. RESULTS AND DISCUSSION

The simulations are conducted on a three-lane road with the settings detailed in Tables I and II. As shown in Fig. 1, the location of each vehicle in Table II represents the coordinate of the vehicle midpoint. In Case I, a typical vehicle-to-vehicle communication scenario, both the Tx and Rx are located in lane 2, and interference arises from the neighboring lanes. In Case II, the Tx and Rx are located in lane 1, and closer than in Case I. Owing to the increased propagation distance and wider irradiance angle, interference from non-adjacent lanes is diminished compared to that from adjacent lanes, resulting in reduced total interference compared to Case I. In contrast to Case I, the distance between the Tx and Rx is increased, while IVs are closer to the Rx in Case III. In the mobility scenario, $h_{att,pq}$ can be estimated based on sensor data, allowing the proposed method to remain applicable in calculating the EC during vehicle mobility.

The CDF of SINR under varying AT strengths is plotted in Fig. 2, while the vehicle locations conform to Case I. An increase in σ_{tur}^2 corresponds to a strengthening of AT strength, resulting in an expansion of the SINR value range. The CDF curves illustrate that the SINR in MIMO-based VVLC can be effectively approximated by a log-normal RV with parameters calculated by the proposed WTA method.

In Fig. 3, the CDF of channel capacity under diverse AT strengths is demonstrated, with the vehicle locations conforming to Case I. Under diverse AT strengths, the derived probability distribution of channel capacity closely approximates the results obtained by the Monte Carlo method. Strong AT induces more severe power fluctuations in the received optical signal compared to weak AT, resulting in a larger deviation of the SINR from its mean value. Consequently, the channel capacity under strong AT exhibits a more widely dispersed probability distribution than that under weak AT.

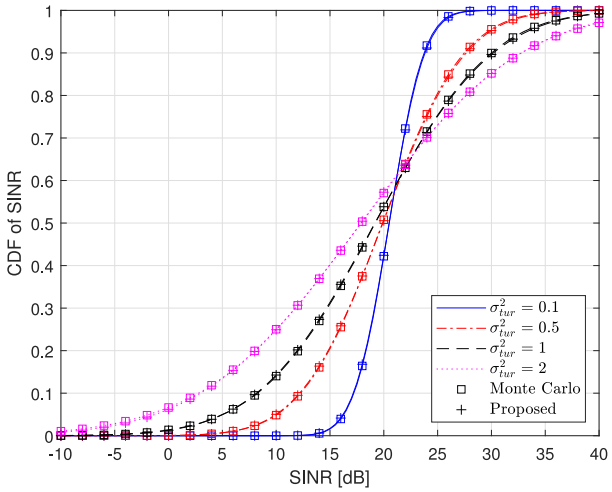

Fig. 2. The CDF of SINR under different AT strengths.

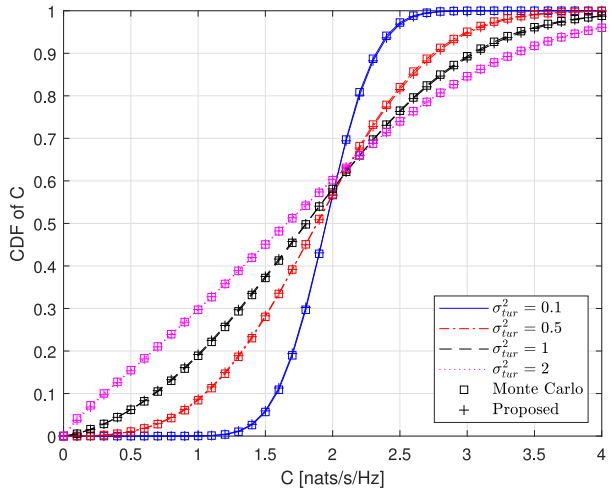

Fig. 3. The CDF of channel capacity under different AT strengths.

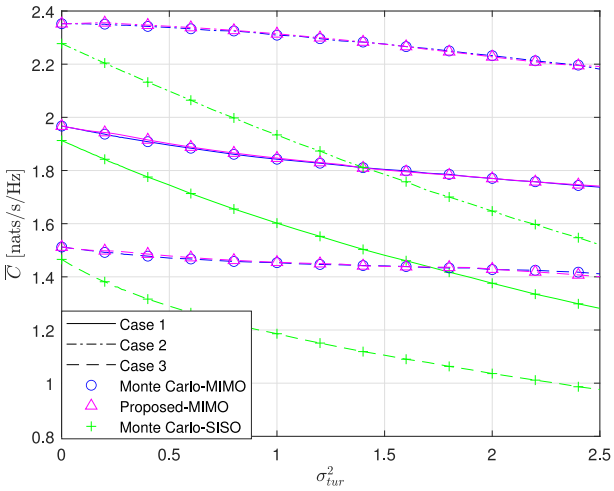

Fig. 4. The variation of the EC with respect to AT strength.

The EC for different AT strengths is displayed in Fig. 4, with n in (24) selected as 20. The results reveal that the MIMO-based VVLC yields a higher EC than the single-input single-output (SISO) VVLC, especially in strong AT scenarios, which affirms the potential of MIMO-based VVLC

$$\mathrm{Cov}\left(\beta_{pq,i},\beta_{p'q',i'}\right)=\begin{cases}\exp\left(2\mu_{\beta,pq,T}+\sigma^2_{\beta,pq,T}\right)\left(e^{\sigma^2_{\beta,pq,T}}-1\right), & \text{if } p=p' \text{ and } q=q' \text{ and } i=i',\\ \exp\left(\mu_{\beta,pq,i}+\mu_{\beta,p'q',i'}+\frac{\sigma^2_{\beta,pq,i}+\sigma^2_{\beta,p'q',i'}}{2}\right)\left(e^{\sigma^2_{\alpha}}-1\right), & \text{otherwise.}\end{cases} \tag{29}$$

$$\mathbb{D}[\beta]=\sum_{p=1}^{N_t}\sum_{q=1}^{N_r}\sum_{p'=1}^{N_t}\sum_{q'=1}^{N_r}\sum_{i=1}^{N_{pq}}\sum_{i'=1}^{N_{p'q'}}\mathrm{Cov}\left(\beta_{pq,i},\beta_{p'q',i'}\right)+\sum_{p=1}^{N_t}\sum_{q=1}^{N_r}\sum_{i=1}^{N_{pq}}\exp\left[\mu_{\beta,pq,i}+\mu_{\beta,0}+\frac{\sigma^2_{\beta,pq,i}+\sigma^2_{\beta,0}}{2}\right]\left(e^{\sigma^2_{\alpha}}-1\right). \tag{30}$$

in mitigating the negative effects arising from AT. In addition, the EC calculated by the GHQ approximates the Monte Carlo results well. Since both signal and interference are influenced by AT, both the numerator and denominator of the SINR fluctuate with the variation of AT strength, thus the variation trend of EC is comprehensively determined by the AT influence on signal and interference. Compared to Case I, the VVLC attains a higher EC in Case II, owing to the closer distance between Tx and Rx, coupled with a lower total interference experienced by the Rx. Conversely, in Case III, the increase in the distance between Tx and Rx leads to a decrease in SINR, resulting in a smaller EC than that in Case I.

VI. Conclusion

In this letter, MIMO-based VVLC is employed to resist the negative impacts caused by AT. Under the influence of AT, the SINR of MIMO-based VVLC becomes an RV, whose closed-form PDF is challenging to formulate. According to the proposed WTA method, SINR can be approximated by a log-normal RV. Based on this approximation, the EC is calculated by GHQ. The simulation results demonstrate that the PDFs of SINR and channel capacity become more dispersed as the AT gradually strengthens. Under different AT strengths, the effectiveness of the proposed WTA method and the EC calculation method is proved by the simulation results. Moreover, the simulation results confirm the potential of MIMO-based VVLC in enhancing EC in the presence of AT, especially in strong AT scenarios.

Appendix

The Central Moment of α and β

Based on (7) and (8), the expectation and variance of α are calculated as

$$\mathbb{E}[\alpha]=\sum_{p=1}^{N_t}\sum_{q=1}^{N_r}e^{\mu_{\alpha,pq,T}+\frac{\sigma^2_{\alpha,pq,T}}{2}}, \tag{26}$$

$$\mathbb{D}[\alpha]=\sum_{p=1}^{N_t}\sum_{q=1}^{N_r}e^{2\mu_{\alpha,pq,T}+\sigma^2_{\alpha,pq,T}}\left(e^{\sigma^2_{\alpha,pq,T}}-1\right). \tag{27}$$

According to (7), the expectation of β is represented as

$$\mathbb{E}[\beta]=\sum_{p=1}^{N_t}\sum_{q=1}^{N_r}\sum_{i=1}^{N_{pq}}e^{\mu_{\beta,pq,i}+\frac{\sigma^2_{\beta,pq,i}}{2}}+e^{\mu_{\beta,0}+\frac{\sigma^2_{\beta,0}}{2}}. \tag{28}$$

Considering the correlation among $\beta_{pq,i}$, the correlation coefficients are derived first in (29), shown at the top of the page, and then $\mathbb{D}[\beta]$ is calculated in (30) at the top of the page.

References

[1] A. Memedi and F. Dressler, "Vehicular visible light communications: A survey," *IEEE Commun. Surveys Tuts.*, vol. 23, no. 1, pp. 161–181, 1st Quart., 2021.

[2] A.-M. Cailean and M. Dimian, "Current challenges for visible light communications usage in vehicle applications: A survey," *IEEE Commun. Surveys Tuts.*, vol. 19, no. 4, pp. 2681–2703, 4th Quart., 2017.

[3] M. Karbalayghareh, F. Miramirkhani, H. B. Eldeeb, R. C. Kizilirmak, S. M. Sait, and M. Uysal, "Channel modelling and performance limits of vehicular visible light communication systems," *IEEE Trans. Veh. Technol.*, vol. 69, no. 7, pp. 6891–6901, Jul. 2020.

[4] P. Sharda, G. S. Reddy, M. R. Bhatnagar, and Z. Ghassemlooy, "A comprehensive modeling of vehicle-to-vehicle based VLC system under practical considerations, an investigation of performance, and diversity property," *IEEE Trans. Commun.*, vol. 70, no. 5, pp. 3320–3332, May 2022.

[5] X. Fu, C. Guo, Y. Qu, and X.-H. Lin, "Resource allocation and blocklength selection for low-latency vehicular communications," *IEEE Wireless Commun. Lett.*, vol. 10, no. 5, pp. 914–918, May 2021.

[6] L. An, H. Shen, J. Wang, Y. Zeng, and R. Ran, "Energy efficiency optimization for MIMO visible light communication systems," *IEEE Wireless Commun. Lett.*, vol. 9, no. 4, pp. 452–456, Apr. 2020.

[7] F. Xing, S. He, Y. Yue, and H. Yin, "Ergodic rate characterization for rate-splitting multiple access based underwater wireless optical communications," in *Proc. 95th Veh. Technol. Conf. (VTC-Spring)*, Helsinki, Finland, Jun. 2022, pp. 1–7.

[8] O. Narmanlioglu, B. Turan, S. C. Ergen, and M. Uysal, "Cooperative MIMO-OFDM based inter-vehicular visible light communication using brake lights," *Comput. Commun.*, vol. 120, pp. 138–146, May 2018.

[9] C. Tebruegge, A. Memedi, and F. Dressler, "Reduced multiuser-interference for vehicular VLC using SDMA and matrix headlights," in *Proc. IEEE Global Commun. Conf. (GLOBECOM)*, Waikoloa, HI, USA, Dec. 2019, pp. 1–6.

[10] Z. Ghassemlooy, W. Popoola, and S. Rajbhandari, *Optical Wireless Communications: System and Channel Modelling With MATLAB*, 2nd ed. Boca Raton, FL, USA: CRC Press/Taylor & Francis Group, 2018.

[11] S. C. Schwartz and Y. S. Yeh, "On the distribution function and moments of power sums with log-normal components," *Bell Syst. Tech. J.*, vol. 61, no. 7, pp. 1441–1462, Sep. 1982.

[12] N. B. Mehta, J. Wu, A. F. Molisch, and J. Zhang, "Approximating a sum of random variables with a lognormal," *IEEE Trans. Wireless Commun.*, vol. 6, no. 7, pp. 2690–2699, Jul. 2007.

[13] A. Safak, "Statistical analysis of the power sum of multiple correlated log-normal components," *IEEE Trans. Veh. Technol.*, vol. 42, no. 1, pp. 58–61, Feb. 1993.

[14] M. Obeed, A. M. Salhab, M.-S. Alouini, and S. A. Zummo, "On optimizing VLC networks for downlink multi-user transmission: A survey," *IEEE Commun. Surveys Tuts.*, vol. 21, no. 3, pp. 2947–2976, 3rd Quart., 2019.

[15] A. Lapidoth, S. M. Moser, and M. A. Wigger, "On the capacity of free-space optical intensity channels," *IEEE Trans. Inf. Theory*, vol. 55, no. 10, pp. 4449–4461, Oct. 2009.